

Aspects of Intervalence Charge Transfer in Cyanide-Bridged Systems: Modulated Electric Field Assessment of Distances, Polarizability Changes, and Anticipated First Hyperpolarizability Characteristics

Fredrick W. Vance,* Laba Karki, James K. Reigle, Joseph T. Hupp,*[†] and Mark A. Ratner

Department of Chemistry and Materials Research Center, Northwestern University, Evanston, Illinois 60208

Received: March 2, 1998; In Final Form: June 2, 1998

Electroabsorption studies of the systems $(\text{CN})_5\text{M}^{\text{II}}-\text{CN}-\text{M}'^{\text{III}}(\text{NH}_3)_5^{1-}$ ($\text{M} = \text{Fe}, \text{Ru}, \text{Os}$; $\text{M}' = \text{Ru}, \text{Os}$) reveal that the metal-to-metal or intervalence charge-transfer transitions are associated with a change in dipole moment, $|\Delta\mu|$, ranging from 11 to 17 D. This change corresponds to a charge-transfer distance of ca. one-half to two-thirds of the geometric separation between the donor and acceptor metals. This result has consequences for electron transfer parameters, where electronic coupling energies are now upwardly revised to as high as 3000 cm^{-1} . The result is also pertinent in the context of nonlinear optics, where $\Delta\mu$ can be utilized in a two level model to estimate wavelength-dependent molecular first hyperpolarizabilities. The change in polarizability ($\Delta\alpha$) accompanying the optical intervalence transitions varies from -10 to $+310 \text{ \AA}^3$. Comparing the experimental results to a simple two state model suggests that the two state picture is seriously deficient for these systems and that a multitude of available additional states must be included to achieve a quantitative description of the polarizable intervalence excited states of these systems.

Introduction

Among the most fundamental quantities in electron-transfer (ET) processes is the distance the electron travels. Elucidation of the ET distance has been the focus of several research efforts involving electroabsorption, or Stark, spectroscopy.^{1,2} Results from our lab and others have shown that, for many bridged inorganic donor/acceptor transfer transitions, the effective charge transfer distance is significantly smaller than the geometric separation of donor and acceptor centers. The difference can have a profound effect on the way in which other important quantities, such as the solvent reorganization energy and the initial state/final state electronic coupling energy are modeled.

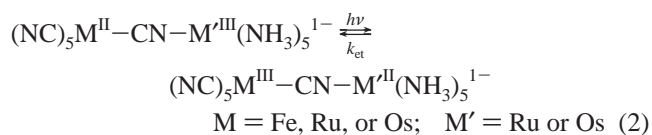
Charge-transfer distances also contribute in an interesting way to the efficiencies of certain nonlinear optical processes. For example, nonresonant frequency doubling processes, which can be viewed in the two-level limit as virtual optical electron-transfer processes,³ exhibit first hyperpolarizabilities (β) that scale as the virtual charge-transfer distance R . In the limit of zero frequency, they are given by

$$\beta_0 = \frac{3\pi e^2 f e R}{hmE_{\text{op}}^3} = \frac{3\pi e^2 f \Delta\mu}{hmE_{\text{op}}^3} \quad (1)$$

In eq 1, f is the oscillator strength for charge-transfer absorption, e is the unit electronic charge, E_{op} is the energy of the absorption maximum, $\Delta\mu$ is the change in dipole moment, h is Planck's constant, and m is the electron mass.

The focus of this work is on the evaluation of charge transfer distances for several members of a family of mixed valence systems known to exhibit both interesting ultrafast electron-

transfer behavior (eq 2)⁴ and promising second-order nonlinear optical (NLO) behavior.⁵



We then seek to use the distance results to understand and predict further aspects of both kinds of behavior. As shown in Figure 1, the target compounds are characterized by intense metal-to-metal or intervalence charge-transfer transitions in the visible and/or near-infrared region, but are otherwise spectrally simple—implying that two-level/two-state analyses may indeed be useful. Preliminary reports for two members of the series have already appeared.^{2a,b}

Experimental Section

All compounds were synthesized by published methods and isolated as sodium salts.⁶ The solvent glass used was a 1:1 (v:v) solution of ethylene glycol:water for visible region studies or ethylene glycol:D₂O for studies in the near-infrared region. The electroabsorption measurements were conducted at 77 K in a manner described previously,² with the additional use of a silicon photodiode for detection in the near-infrared region.

Results

Figure 2 shows a representative set of linear absorption and electroabsorption spectra, in this case for $(\text{NC})_5\text{Fe}-\text{CN}-\text{Ru}(\text{NH}_3)_5^{1-}$ (**1**). The data were interpreted by following Liptay's analysis⁷ whereby the electroabsorption signal $\Delta A(\nu)$ is fit to a

[†] jthupp@chem.nwu.edu.

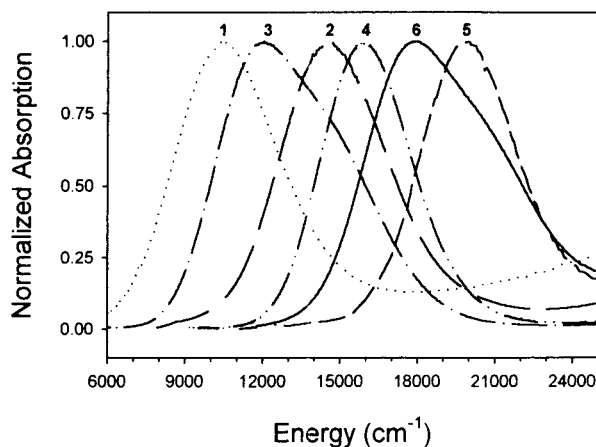


Figure 1. Room-temperature absorption spectra (normalized) showing MMCT bands of compounds **1–6** in unbuffered water as solvent. **1** = $(\text{CN})_5\text{Fe}^{\text{II}}\text{CNRu}^{\text{III}}(\text{NH}_3)_5^{1-}$, **2** = $(\text{CN})_5\text{Ru}^{\text{II}}\text{CNRu}^{\text{III}}(\text{NH}_3)_5^{1-}$, **3** = $(\text{CN})_5\text{Os}^{\text{II}}\text{CNRu}^{\text{III}}(\text{NH}_3)_5^{1-}$, **4** = $(\text{CN})_5\text{Fe}^{\text{II}}\text{CNOs}^{\text{III}}(\text{NH}_3)_5^{1-}$, **5** = $(\text{CN})_5\text{Ru}^{\text{II}}\text{CNOs}^{\text{III}}(\text{NH}_3)_5^{1-}$, **6** = $(\text{CN})_5\text{Os}^{\text{II}}\text{CNOs}^{\text{III}}(\text{NH}_3)_5^{1-}$.

linear combination of zeroth, first, and second derivatives of the absorption band $A(\nu)$:

$$\Delta A(\nu) = \left\{ A_\chi A(\nu) + \frac{B_\chi \nu}{15hc} \frac{d[A(\nu)/\nu]}{d\nu} + \frac{C_\chi \nu}{30h^2 c^2} \frac{d^2[A(\nu)/\nu]}{d\nu^2} \right\} \mathbf{F}_{\text{int}}^2 \quad (3)$$

In eq 3, \mathbf{F}_{int} is the internal electric field,⁸ ν is the frequency of the absorbed light, and c is the speed of light. The resulting coefficients A_χ , B_χ , and C_χ have been described in detail previously.^{1c} Briefly, however, they provide information, respectively, about changes in the transition moment, the molecular polarizability, and the permanent dipole moment.

The dominance of the second derivative term, and thus C_χ , in the fits of electroabsorption spectra for compounds **1–6** (see Table 1 for numbering scheme) indicates that most of the Stark intensity arises from changes in dipole moment between the ground and excited electronic states $\Delta\mu_{12}$. The dipole moment information readily yields the effective (adiabatic) charge-transfer distance R_{12} :

$$R_{12} \equiv \frac{\Delta\mu_{12}}{e} \quad (4)$$

Notably, the values obtained (2.4–3.5 Å;^{9–11} Table 1) are small in comparison to the geometric metal–metal separation distance of 5.0 Å.¹²

When Os^{II} is the donor, the spectroscopy becomes more complicated because spin–orbit coupling allows the transition from the d_{xy} orbital (which is nominally orthogonal to the charge-transfer axis z) to gain significant intensity. For these compounds (**3** and **6**), the angle ζ between the transition dipole moment and the change in dipole moment vectors is found to be 10° (**3**) and 22° (**6**) for the overall (sum) transition.¹³ These are marginally greater than the approximately zero angular dependence found for charge transfer in the other compounds.

From the B_χ coefficient of eq 3, the electroabsorption measurements also yield quantitative information about the trace of the change in polarizability, $\text{Tr}(\Delta\alpha)$. This can be seen from eq 5:¹⁴

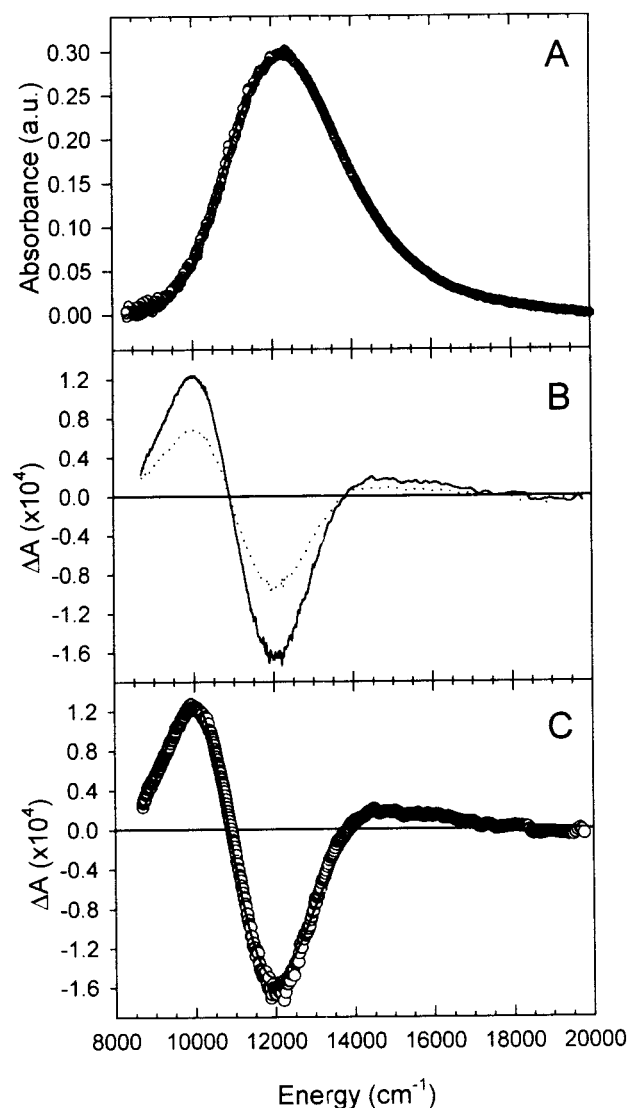


Figure 2. (A) Low-temperature absorption of **1** (circles) with Gaussian fit (line). (B) Stark spectra at 55° (solid) and 90° (dashed). (C) Least-squares fit (line) of 55° data (circles) to eq 3.

$$B_\chi = \frac{5}{2} \text{Tr}(\Delta\alpha) + (3 \cos^2 \chi - 1) \left(\frac{3 \mathbf{m} \cdot \Delta\alpha \cdot \mathbf{m}}{2 |\mathbf{m}|^2} - \frac{1}{2} \text{Tr}(\Delta\alpha) \right) + \frac{1}{|\mathbf{m}|^2} \sum_{ij} [10m_i \alpha_{ij} \Delta\mu_j + (3 \cos^2 \chi - 1)(3m_i \alpha_{ji} \Delta\mu_j + 3m_i \alpha_{ij} \Delta\mu_i - 2m_i \alpha_{ij} \Delta\mu_j)] \quad (5)$$

Here, \mathbf{m} is the transition moment vector, $\Delta\alpha$ and α are respectively the change in polarizability between ground and excited states and the transition polarizability, and χ defines the experimental angle between the incident light and the applied electric field. Although eq 5 contains terms involving the product of α and $\Delta\mu$, these terms are often negligible, and thus the assumption is often made that the $\text{Tr}(\Delta\alpha)$ contribution dominates B_χ . Alternatively, a two level model can be used to predict the magnitude of the product terms.^{1a} Doing so under the appropriate experimental condition where $\chi = 54.7^\circ$ reduces the expression to two terms which can be simplified as in eq 6:

$$B_\chi = \frac{5}{2} \text{Tr}(\Delta\alpha) + \frac{10(\Delta\mu)^2}{E_{\text{op}}} \quad (6)$$

Presented in Table 1 for compounds **1–6** are estimates for

TABLE 1: Linear Absorption and Electroabsorption Properties for (NC)₅M^{II}–CN–M^{III}(NH₃)₅¹⁻ Species at 77K

compound	E_{op} (cm ⁻¹)	$\Delta\nu_{1/2}$ (cm ⁻¹)	μ_{12}^a (eÅ)	$ \Delta\mu_{12} $ (D)	R_{12} (Å)	$\text{Tr}(\Delta\alpha)^b$ (Å ³)	$\text{Tr}(\Delta\alpha)^c$ (Å ³)	$\Delta\alpha(\text{calcd})^d$ (Å ³)
1. Fe(II)–Ru(III)	12200	2860	0.77	11.5	2.4	230	10	11
2. Ru(II)–Ru(III)	16100	3650	0.63	13.4	2.8	450	220	4.9
3. Os(II)–Ru(III)	13200 ^e	3200	0.42	16.8	3.5	480	60	6.7
4. Fe(II)–Os(III)	17800 ^f	3400 ^f	0.44	12.5 ^f	2.6 ^f	170 ^f	-10	3.8
5. Ru(II)–Os(III)	21600	3530	0.42	13.4	2.8	340	170	2.8
6. Os(II)–Os(III)	19100	3830	0.40	14.9	3.1	250	20	2.9

^a Determined from room-temperature absorption spectra. ^b Evaluated via eq 5 by neglecting all product terms. ^c Evaluated via eq 6. ^d Calculated from eqs 14 and 15. ^e From ref 2b. ^f From ref 2a.

TABLE 2: Quantities Calculated from the Adiabatic Charge Transfer Distance, R_{ab}

compound	R_{ab} (Å)	c_b^2	H_{ab} (cm ⁻¹)	$\beta_0 \times 10^{30}$ (esu) ^b	$\beta_{1064} \times 10^{30}$ (esu) ^b
1. Fe(II)–Ru(III)	2.8	0.079	2800	-38	97
2. Ru(II)–Ru(III)	3.0	0.039	3000	-14	37
3. Os(II)–Ru(III)	3.7	0.029	1300 ^e	-14	25
4. Fe(II)–Os(III)	2.8	0.038	2500	-5.6	22
5. Ru(II)–Os(III)	3.0	0.030	2850	-3.3	-28
6. Os(II)–Os(III)	3.2	0.024	2100 ^e	-5.0	30

^a See ref 11. ^b From eq 11.

$\text{Tr}(\Delta\alpha)$ obtained from eq 5 by assuming that all product terms can be neglected. Also listed are estimates derived instead from eq 6. From either data set, the following patterns are evident: (a) replacement of Os^{III} (4–6) by Ru^{III} (1–3) as the electron acceptor yields an increase in the polarizability change and (b) replacement of Fe^{II} (1, 4) by Ru^{II} (2, 5) as the electron donor yields an increase in $\text{Tr}(\Delta\alpha)$.

Discussion

Changes in Dipole Moment: General Trends. Perhaps the most surprising experimental observation is that substitution of the donor or acceptor metal center, or both, produces only modest changes in $|\Delta\mu_{12}|$ and in the effective one-electron-transfer distances. This suggests that variable factors such as electronegativity and d-orbital extension are less significant than constant factors such as total charge, valence electron count, orbital occupancy, geometry, and ligand field strength.

Electron-Transfer Implications. Among the factors of interest in an electron-transfer process is the amount of localization or delocalization present in the reactive system. One way to assess delocalization is to compare the adiabatic charge-transfer distance R_{12} to the diabatic charge-transfer distance R_{ab} found from eqs 7¹⁵ and 8:¹⁶

$$\Delta\mu_{\text{ab}} = eR_{\text{ab}} = [(\Delta\mu_{12})^2 + 4\mu_{12}^2]^{1/2} \quad (7)$$

$$\mu_{12} = 2.07 \times 10^{-2} \left(\frac{\epsilon_{\text{max}} \Delta\nu_{1/2}}{E_{\text{op}} b} \right)^{1/2} \quad (8)$$

Here ϵ_{max} is the molar extinction coefficient in cm⁻¹M⁻¹, $\Delta\nu_{1/2}$ is the absorption bandwidth (full width at half-maximum) in cm⁻¹, E_{op} is the absorption band maximum in cm⁻¹, and b is the degeneracy of the transition. The primary transitions studied here arise from electron transfer from either M^{II}(d_{xz}) or M^{II}(d_{yz}) (degenerate orbitals) suggesting a degeneracy of two. However, since the M^{III} center has only one available accepting site (either a d_{xz} or a d_{yz}), the effective degeneracy of the transition is one.¹⁷ In compounds 3 and 6, the additional transition allowed by spin-orbit coupling to the Os^{II} d_{xy} orbital likewise has a degeneracy of unity.¹⁸

As shown in Table 2, the six mixed valence compounds exhibit diabatic charge transfer distances that are only marginally greater (≤ 0.4 Å) than the corresponding adiabatic distances. Thus, delocalization clearly is *not* the primary factor responsible for the observed “shorter than geometric” electron-transfer distances. (Recall that the diabatic distance is the electron-transfer distance that would be obtained under hypothetical conditions of zero electronic coupling.¹⁶) In any case, the diabatic and adiabatic electron-transfer distances or dipole moment changes can subsequently be combined to yield the degree of delocalization as expressed by the Hush mixing coefficient c_b^2 .^{2,1a,16}

$$c_b^2 = \frac{1}{2} \left[1 - \left(\frac{\Delta\mu_{12}^2}{\Delta\mu_{12}^2 + 4\mu_{12}^2} \right)^{1/2} \right] = \frac{1}{2} \left[1 - \frac{\Delta\mu_{12}}{\Delta\mu_{\text{ab}}} \right] \quad (9)$$

Recall that a c_b^2 value of zero corresponds to complete localization and that a c_b^2 value of 0.5 corresponds to complete delocalization. In addition, for a two-state system where direct donor/acceptor orbital overlap can be neglected, the quantity $(1 - 2c_b^2)e$ describes the effective amount of charge transferred based on diabatic initial and final electronic states. For all the transitions considered here, $c_b^2 < 0.08$ and $(1 - 2c_b^2) > 0.84$ (Table 2).

Once the diabatic charge-transfer distance is known, eq 10 can be used to calculate the electronic coupling matrix element H_{ab} , where E_{op} is now the absorption maximum (cm⁻¹) at room temperature:¹⁵

$$H_{\text{ab}} = \frac{\mu_{12} E_{\text{op}}}{eR_{\text{ab}}} \quad (10)$$

As shown in Table 2, the values obtained for H_{ab} are similar for all compounds studied, implying that the structural and chemical commonalities within this family define the dominant effects. It should also be noted that the H_{ab} values are as much as a factor of 2 larger than implied by calculations based on purely geometric donor/acceptor separation distances. We have noted elsewhere² that the increases in H_{ab} may have implications in terms of ET reaction dynamics and should also have significant consequences in terms of potential energy surface shapes, particularly in the vicinity of ET reaction related curve crossings.

NLO Implications. Electroabsorption spectroscopy can also be exploited in the rational design of nonlinear optical (NLO) chromophores, or perhaps more realistically in the *rationalization* of the responses from existing chromophores. Because the electroabsorption experiment readily yields $|\Delta\mu_{12}|$,¹⁹ the combination of this experiment and a conventional linear absorption experiment provides sufficient information for implementation of a two-level/two-state calculation of the first hyperpolarizability along the charge-transfer axis β_{ct} . The relevant equations are^{3,16}

$$\beta_{\text{ct}} = \frac{3e^2 E_{\text{op}} f_{12} \Delta\mu_{12}}{2\hbar m [(E_{\text{op}})^2 - (2E_{\text{inc}})^2][(E_{\text{op}})^2 - (E_{\text{inc}})^2]} \quad (11)$$

$$f_{12} = 4.61 \times 10^{-9} \Delta\nu_{1/2} \epsilon_{\text{max}} \quad (12)$$

Here E_{inc} is the incident one-photon energy and the required values for ϵ_{max} , $\Delta\nu_{1/2}$, and E_{op} are now taken from room-temperature absorption spectra. Note that the sign of $\Delta\mu_{12}$ must be inferred from chemical considerations, because the experiment yields only the absolute value. Consistent with eq 2, it was taken as negative for all transitions considered here.

On the basis of the calculated hyperpolarizabilities summarized in Table 2, at least two observations are worth mentioning. First, in the zero frequency limit ($E_{\text{inc}} = 0$) a modest inverse correlation is observed between the absolute value of β_{ct} (calcd) and the MMCT transition energy (cf. eq 1). Second, the calculation of 14×10^{-30} esu for $|\beta_0(\mathbf{2})|$ falls below the value of 81×10^{-30} esu suggested by Laidlaw and co-workers based on extrapolation from the experimental results obtained at $E_{\text{inc}} = 1064$ nm;^{5,20} the estimate is also smaller than the reported two-level computational result of 41×10^{-30} esu from the same work.^{5,21} The latter difference is primarily due to the substantial difference between the measured electron-transfer distance and the geometric separation distance (used in the earlier work).²² The discrepancy between calculated $|\beta_0(\mathbf{2})|$ (Table 2) and extrapolated experimental $|\beta_0(\mathbf{2})|$ values, on the other hand, is more puzzling. "Improvement" of the former by inclusion of higher excited states and the addition of three-level effects is unlikely to narrow the discrepancy. Indeed, consideration of these effects typically lowers β_0 (calcd) values.²³ We suggest instead that the origin of the discrepancy may be in the protocol used to extrapolate finite-frequency experimental data to $E_{\text{inc}} = 0$. In ref 21 (as well as in most other studies), expressions similar to eq 11 are used. These are anticipated to be reasonably accurate when measurements and extrapolations both take place far from resonance. Closer to resonance, however, expressions such as eq 11 typically underestimate β_{ct} and, therefore, overestimate $\beta_0/\beta_{\text{ct}}$ because they assume that electronic transitions are infinitely narrow. Alternative expressions exist which take into account the effects of uncertainty or lifetime broadening.^{24,25} The potentially much more significant effects of vibrational and solvational (Franck–Condon) broadening, however, have not, to the best of our knowledge, been treated in existing studies. Qualitatively, however, inclusion of Franck–Condon broadening will amplify the effects of electronic resonance when incident (or doubled incident) energies are significantly displaced from E_{op} yet involve finite absorption cross sections. This is precisely the circumstance encountered for $\mathbf{2}$ with $E_{\text{op}} = 14600$ cm^{-1} , $E_{\text{inc}} = 9400$ cm^{-1} , and $2E_{\text{inc}} = 18800$ cm^{-1} : Under these conditions, $\epsilon(E_{\text{op}}) = 2800$ $\text{M}^{-1}\text{cm}^{-1}$, $\epsilon(E_{\text{inc}}) = 140$ $\text{M}^{-1}\text{cm}^{-1}$ and $\epsilon(2E_{\text{inc}}) = 620$ $\text{M}^{-1}\text{cm}^{-1}$ (cf. Figure 1). As suggested by Figure 3, these effects may become very important under near resonant conditions, such as those used in NLO experiments for compound $\mathbf{2}$.

Changes in Polarizability. In contrast to changes in dipole moment, changes in polarizability, as measured by the trace, $\text{Tr}(\Delta\alpha)$, are highly dependent on the identity of the metal centers engaging in intervalence transfer. To understand the experimental observations, descriptions of both ground and excited-state polarizabilities are needed. As a first step toward these descriptions, it is useful to consider a sum-over-states expression. A simplified representation of the static first-order polarizability for an arbitrary electronic state n (one-dimensional case) is shown in eq 13:²⁵

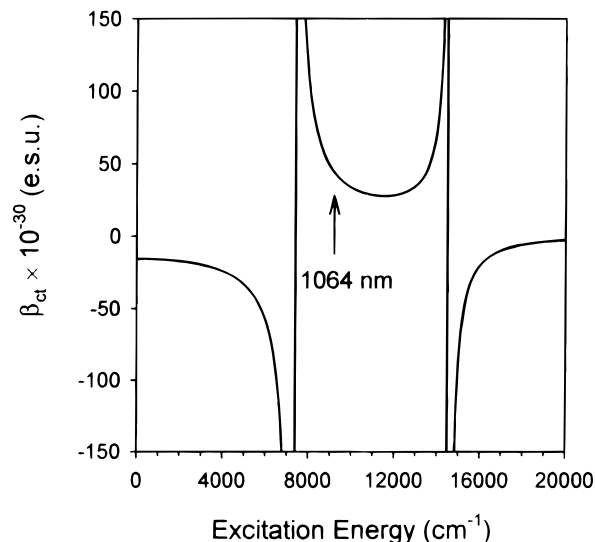


Figure 3. Calculated dependence of β on excitation energy for compound $\mathbf{2}$, using the two-level model of eq 11. Notice that only the real portion of β has been plotted. Including the imaginary portion would remove the discontinuities plotted. As shown, excitation at 1064 nm (9400 cm^{-1}) falls near the two photon resonance (centered at 7300 cm^{-1}). Thus, the discrepancy between the model and experiment may be due to the exclusion of damping and Franck–Condon broadening terms which would expand the region over which significant resonance enhancement would be expected.

$$\alpha_n = 2 \sum_{m \neq n} \frac{\langle n|\mu|m\rangle\langle m|\mu|n\rangle}{E_{nm}} \quad (13)$$

Here $\langle n|\mu|m\rangle$, which can also be denoted μ_{nm} , refers to the electronic transition dipole moment between states n and m . If the summation is limited to two states, where the ground state is 1 and the excited state is 2, the expression for the polarizability of each state is eq 14:

$$\alpha_1 = -\alpha_2 = 2 \frac{\mu_{12}^2}{E_{12}} \quad (14)$$

This leads directly to eq 15 for the change in polarizability $\Delta\alpha$:

$$\Delta\alpha_{12} = \alpha_2 - \alpha_1 = -2\alpha_1 = 2\alpha_2 \quad (15)$$

These expressions can be evaluated from linear absorption spectroscopy by equating the absorption maximum with E_{12} and using eq 8 to obtain μ_{12} .

The bimetallic compounds in this study undoubtedly contain a large number of states, many of which lie energetically close to the first excited state. The two-level/two-state description would be expected to fail if these additional states can also contribute to the observed changes in polarizability. Indeed, when the experimental values of $\text{Tr}(\Delta\alpha)$ are compared to those predicted by eqs 14 and 15 (Table 1) several discrepancies are evident: (a) the sign of $\Delta\alpha(\text{exptl})$ is opposite to that expected based on the two level model, (b) the absolute experimental values of $\text{Tr}(\Delta\alpha)$ are 1–2 orders of magnitude larger than predicted by the two-level model, and (c) the compound-to-compound variation is much greater than predicted by the two-level model.

Despite the rather striking quantitative failings, the two-level/two-state model is useful in a qualitative sense for understanding the trends observed for this family of molecules. Table 1 shows, as the model predicts, that, with either electron acceptor, increasing the calculated polarizability of the ground state α_1 ,

by changing the chemical identity of the electron donor (the hexacyanide coordinated site), causes a decrease in $\Delta\alpha$. On the other hand, changing the chemical identity of the electron acceptor (the ammine coordinated site) induces changes in the experimental $\Delta\alpha$ value that are inconsistent with the two state description. This is most likely an indication, as expected, that additional states must be included in the descriptions of the polarizabilities, presumably, a rather large number of additional states, given the substantial discrepancies between $\Delta\alpha(\text{eq 15})$ and $\Delta\alpha(\text{exptl})$. If so, then polarizability changes would appear to be highly sensitive reporters on upper electronic state involvement in intervalence charge transfer processes. In contrast, dipole moment changes appear to be comparatively insensitive to upper excited-state effects.

Conclusions

Electroabsorption spectroscopy is a powerful tool for understanding electron transfer processes. The most striking finding of this study is that changes in the identity of the metal donor and acceptor centers for this family of chromophores exert only minor effects upon the charge transfer character of the electronic transitions as measured by the absolute change in molecular dipole moment. The experiments do show, however, that light-induced electron transfer occurs over effective distances that are only $\sim 60\%$ as large as the crystallographically measured separation distance between donor and acceptor metal ions. For NLO applications, the shortened distances imply lessened participation by the intervalence excited state in frequency doubling processes, and therefore, smaller molecular first hyperpolarizabilities than might otherwise be anticipated. Finally, the change in polarizability, $\text{Tr}(\Delta\alpha)$, was found to vary in a way which is only qualitatively accounted for by a simple two-state description, implying that a multiplicity of higher lying excited states contributes to the polarizabilities of the low lying intervalence excited states for these complexes.

Acknowledgment. We acknowledge helpful discussions with Albert Israel concerning conventions in nonlinear optic calculations. We thank Steve Boxer for a preprint of ref 11 and helpful comments on spectral deconvolution. We thank the U.S. Department of Energy, Office of Research, Division of Chemical Sciences (Grant DE-FG02-87ER13808) and the Materials Research Center at Northwestern University (Grant NSF-DMR-9632472) for support of this research.

References and Notes

- (1) (a) Shin, Y. K.; Brunschwig, B. S.; Creutz, C.; Sutin, N. *J. Phys. Chem.* **1996**, *100*, 8157. (b) Shin, Y. K.; Brunschwig, B. S.; Creutz, C.; Sutin, N. *J. Am. Chem. Soc.* **1995**, *117*, 8668. (c) Oh, D. H.; Sano, M.; Boxer, S. G. *J. Am. Chem. Soc.* **1991**, *113*, 6880. (d) Oh, D. H.; Sano, M.; Boxer, S. G. *J. Am. Chem. Soc.* **1990**, *112*, 8161. (e) Oh, D. H.; Boxer, S. G. *J. Am. Chem. Soc.* **1989**, *111*, 1130.
- (2) (a) Karki, L.; Lu, H. P.; Hupp, J. T. *J. Phys. Chem.* **1996**, *100*, 15637. (b) Karki, L.; Hupp, J. T. *J. Am. Chem. Soc.* **1997**, *119*, 4070. (c) Karki, L.; Hupp, J. T. *Inorg. Chem.* **1997**, *36*, 3318.
- (3) (a) Oudar, J. L. *J. Chem. Phys.* **1977**, *67*, 446. (b) Oudar, J. L.; Chemla, D. S. *J. Chem. Phys.* **1977**, *66*, 2664.
- (4) (a) Walker, G. C.; Barbara, P. F.; Doorn, S. K.; Dong, Y.; Hupp, J. T. *J. Phys. Chem.* **1991**, *95*, 5712. (b) Reid, P. J.; Silva, C.; Barbara, P. F.; Karki, L.; Hupp, J. T. *J. Phys. Chem.* **1995**, *99*, 2609. (c) Wang, C.; Mohny, B. K.; Williams, R. D.; Petrov, V.; Hupp, J. T.; Walker, G. C. *J. Am. Chem. Soc.* **1998**, accepted.
- (5) (a) Laidlaw, W. M.; Denning, R. G.; Verbeist, T.; Chauchard, E.; Persoons, A. *Nature* **1993**, *365*, 58. (b) Laidlaw, W. M.; Denning, R. G.; Verbeist, T.; Chauchard, E.; Persoons, A. *SPIE Proc.* **1994**, *2143*, 14.
- (6) (a) Vogler, A.; Kisslinger, J. *J. Am. Chem. Soc.* **1982**, *104*, 2311. (b) Vogler, A.; Osman, A. H.; Kunkley, H. *Coord. Chem. Rev.* **1985**, *64*, 159. (c) Vogler, A.; Osman, A. H.; Kunkley, H. *Inorg. Chem.* **1987**, *26*, 2337. (d) Forlano, P.; Baraldo, L. M.; Olabe, J. A.; Della Védova, C. O. *Inorg. Chim. Acta* **1994**, *223*, 37.
- (7) (a) Wortmann, R.; Elich, K.; Liptay, W. *Chem. Phys.* **1988**, *124*, 395. (b) Liptay, W. In *Excited States*; Lim, E. C., Ed.; Academic Press: New York, 1974; Vol 1, pp 129–229.
- (8) F_{int} was assumed to be 1.3 times the externally applied field.^{2b}
- (9) The angle dependence (ζ) of the R_{12} values in compounds **3** and **6** could be as large as 23° . Thus, when viewed as contributions along the charge-transfer axis, the overall variance could be even smaller than reported here.
- (10) For comparison, Bublitz, Laidlaw, Denning, and Boxer (*J. Am. Chem. Soc.* **1998**, in press.) report R_{12} values for **3** of 5.0 \AA ($F_{\text{int}}/F_{\text{ext}}$) and 4.6 \AA ($F_{\text{int}}/F_{\text{ext}}$) based on conventional Stark spectroscopy and higher order Stark spectroscopy, respectively. If the ratio of internal to external fields is taken as 1.3, the resulting R_{12} values are 3.8 and 3.5 \AA , respectively (versus 3.5 \AA in the present study).
- (11) It should be noted that the “donor orbital specific” values previously reported for compound **3** are dependent on the deconvolution methodology employed for both the absorption and electroabsorption spectra. Boxer and co-workers have pointed out (ref 10 and Bublitz, G. U.; Boxer, S. G., private communication) that even for spectra acquired at 77 K , attempted deconvolutions may not be unique. Indeed, they find that satisfactory fits for **3** can be achieved by assigning identical electrooptical parameters to the overlapping transitions. A further indication that deconvolution problems exist is observation of a (presumably artifactual) dependence of the deconvolution outcomes on temperature (77 and 298 K ; Karki and Vance, unpublished data). Thus, in this work, we have reported results from a fit of the total line shape for compounds **3** and **6**. We are optimistic that planned absorption and electroabsorption experiments at near liquid He temperatures will provide spectra that are sufficiently resolved to permit unique deconvolutions.
- (12) Vance, F. W.; Slone, R. V.; Stern, C. S.; Hupp, J. T. Unpublished data from X-ray crystallographic studies.
- (13) The angle ζ between the transition dipole moment and the change in dipole moment vectors can be found by measuring the value of C_ζ at various angles of the electric field, χ , which will behave as (see ref. (c)):

$$C_\zeta = |\Delta\mu|^2 [5 + (3 \cos^2 \chi - 1)(3 \cos^2 \zeta - 1)]$$
- (14) Bublitz, G. U.; Boxer, S. G. *Annu. Rev. Phys. Chem.* **1997**, *48*, 213.
- (15) Cave, R. J.; Newton, M. D. *Chem. Phys. Lett.* **1996**, *249*, 15.
- (16) Creutz, C.; Newton, M. D.; Sutin, N. *J. Photochem. Photobiol. A* **1994**, *82*, 47.
- (17) Available single-crystal X-ray structural results (ref 12) show that the octahedral framework for the M and M' coordination sites are adeptly aligned, implying that the vacant acceptor orbital can overlap efficiently with only one of the two candidate donor orbitals. If one of the octahedra were rotated by ca. 45° along the z-axis, then the acceptor orbital would overlap poorly, but roughly equivalently, with both candidate donor orbitals (i.e., b would be 2). In the absence of the X-ray derived structural information, we assumed in an earlier report^{2b} that a b value of 2 was most appropriate. Conversion to $b = 1$ leads to significantly larger estimates for H_{ab} (eq 10) and c_b^2 (eq 9) and marginally larger values for R_{ab} (eq 7).
- (18) For compounds **3** and **6**, ϵ_{max} , $\Delta\nu_{1/2}$, and E_{op} were taken from fits of the larger, lower energy transition.
- (19) The value of $|\Delta\mu_{12}|$ at room temperature can be calculated from eq 7 where $\Delta\mu_{\text{ab}}$ is presumed to be temperature independent and μ_{12} is calculated from room-temperature data. These were found to differ from the low temperature $|\Delta\mu_{12}|$ values by less than 2%.
- (20) At 1064 nm , the measured β was 209×10^{-30} esu (ref 5b).
- (21) Denning, R. G. In *Advances in Spectroscopy*; Clark, R. J. H., Hester, R. E., Eds.; Wiley: Chichester, 1993; pp 1–60.
- (22) There is also a discrepancy in the convention used (a factor of 2). A full discourse on conventions for NLO can be found in Willetts, A.; Rice, J. E.; Burland, D. M.; Shelton, D. P. *J. Chem. Phys.* **1992**, *97*, 7590.
- (23) For example, see: Kanis, D. R.; Ratner, M. A.; Marks, T. J. *Chem. Rev.* **1994**, *94*, 195 and references therein.
- (24) (a) Di Bella, S.; Fraglia, I.; Marks, T. J.; Ratner, M. A. *J. Am. Chem. Soc.* **1996**, *118*, 12747. (b) Brouyère, E.; Persoons, A.; Brédas, J. L. *J. Phys. Chem.* **1997**, *101*, 4142. (c) Yitzchaik, S.; Di Bella, S.; Lundquist, P. M.; Wong, G. K.; Marks, T. J. *J. Am. Chem. Soc.* **1997**, *119*, 2995.
- (25) Meyers, F.; Marder, S. R.; Pierce, B. M.; Brédas, J. L. *J. Am. Chem. Soc.* **1994**, *116*, 10703.